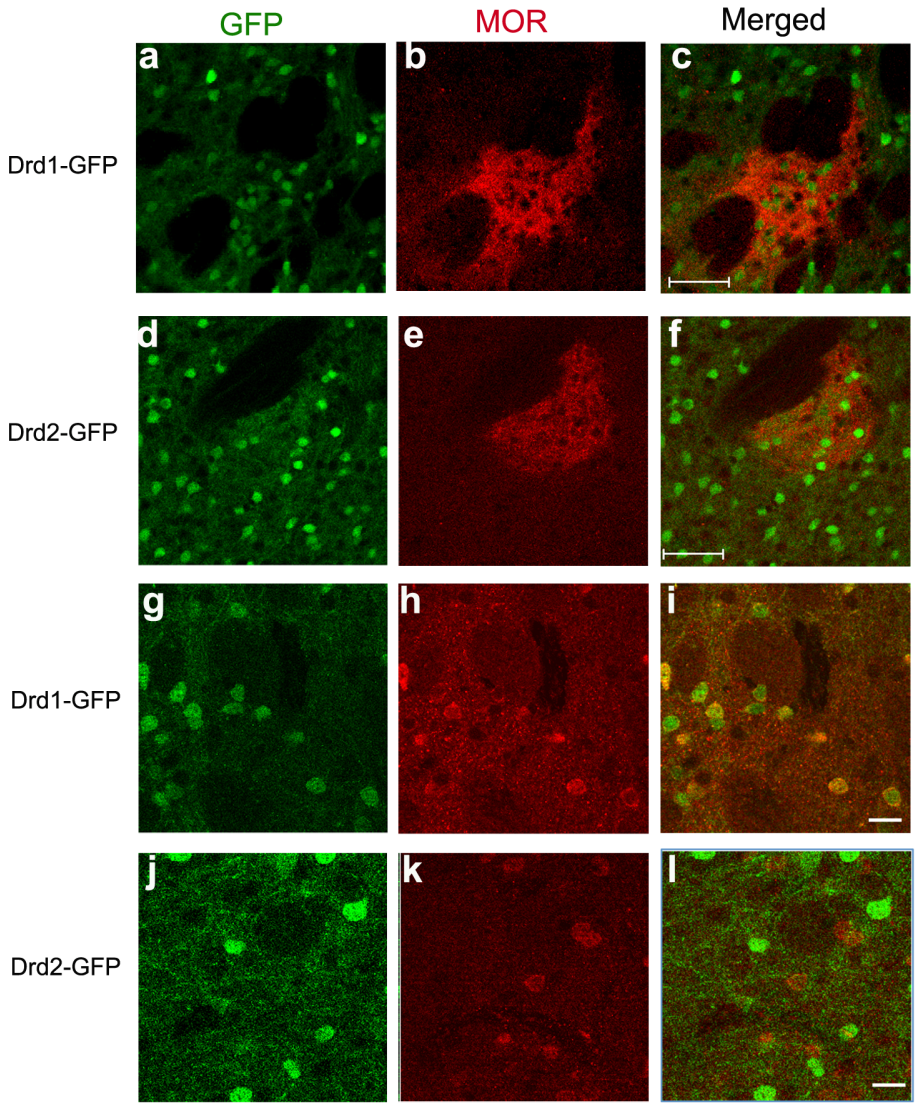


**Supplementary Figure S1.** Immunohistochemical staining of MOR in *Drd1-GFP and Drd2-GFP* mice. **(a-c)** A representative double immunofluorescence staining shows the expression pattern of MOR (red, **b, c**) and GFP (green, **a,c**) in the GENSAT *Drd1-GFP* mouse brain. Scale bar = 50 μm. **(d-f)** A representative double immunofluorescence staining shows the expression pattern on of MOR (red, **e** and **f**) and GFP (green, **d** and **f**) the GENSAT *Drd2-GFP* mouse brain. Scale bar = 50 μm. **(g-i)** A representative double immunofluorescence staining shows the co-localization of MOR (red, **b, c**) and GFP (green, **a,c**) in the GENSAT *Drd1-GFP* mouse brain. Scale bar = 20 μm. **(j-l)** A representative double immunofluorescence staining shows the co-localization of MOR (red, **e** and **f**) and GFP (green, **d** and **f**) the GENSAT *Drd2-GFP* mouse brain. Scale bar = 20 μm.

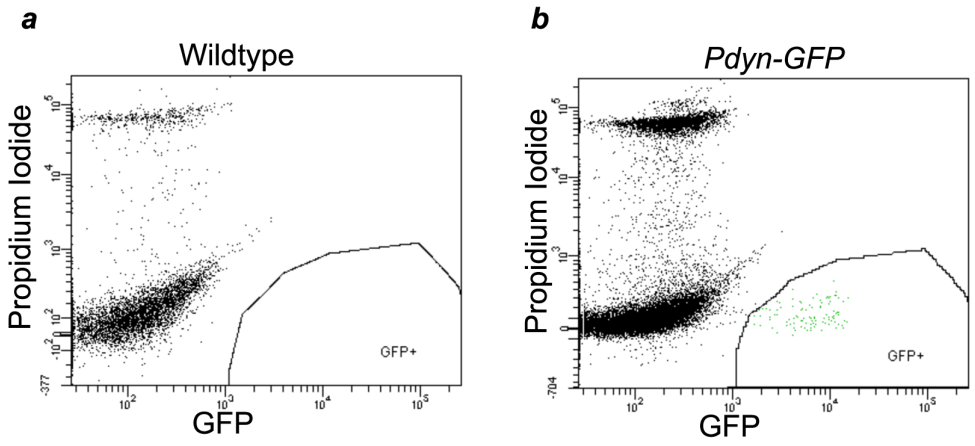


**Supplementary Figure S2.** A example of FACS sorting of the GFP positive but propidium iodide negative neurons from WT (used as negative control) and *Pdyn-GFP* mice. Same gating was used for the *Drd2-GFP* mice. Green dots within the selected area represents the $GFP^{+}$/propidium $iodide^{-}$ cells been collected.

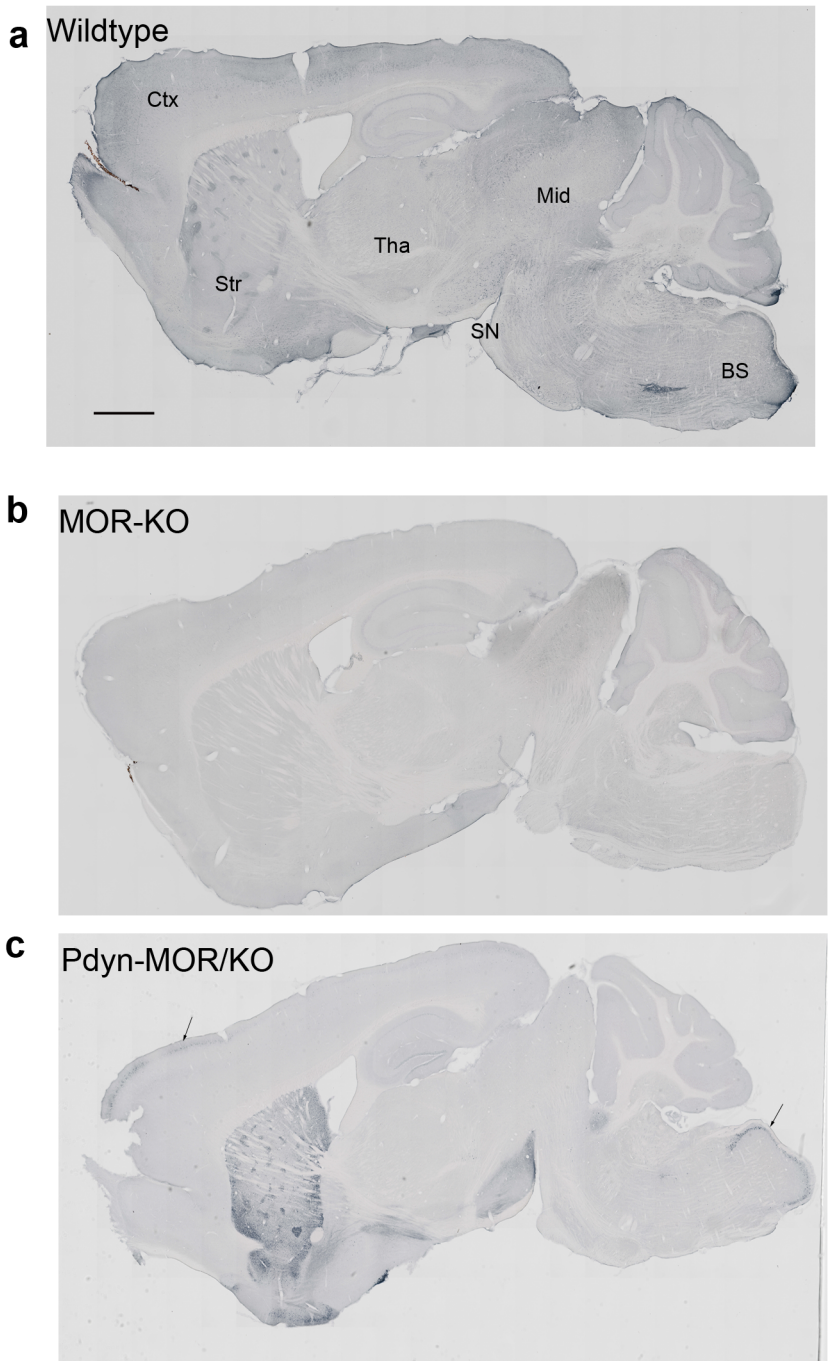


**Supplementary Figure S3.** Immunohistochemical staining of MOR in adult *WT*, *MOR-KO* and *Rescue* mice. (**a**) *WT;* (**b**) *MOR-KO*; and (**c**) *Rescue* mice. The arrows show the expression of MOR in the cortex and brain stem. Ctx, cerebral cortex; Str, striatum; Tha, thalamus; Mid, midbrain, SN, substantia nigra; BS, brain stem. Scare bar = 1 mm.

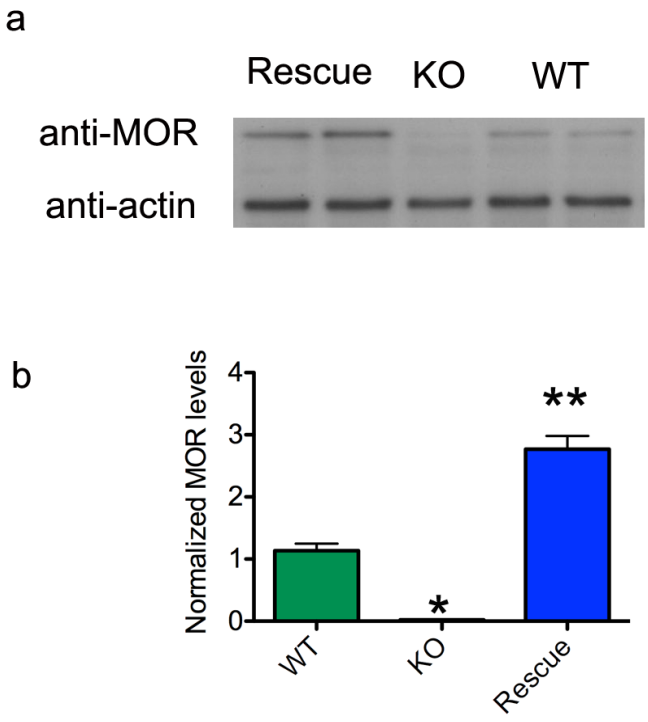


**Supplementary Figure S4.** Western blot analysis of expression of striatal MOR in *Rescue* mice. **(a)** Western blot performed on brain lysates isolated from *Rescue*, *MOR-KO* and WT control mice. **(b)** Quantification of relative MOR expression in the striatum. MOR levels were normalized to those observed in the WT mice ($H_{(2)=}32.143$, $p < 0.001$, Non-parametric one-way ANOVA on ranking; n=4, WT; n=3, *MOR-KO* and n=6, *Rescue*). Values are mean ± SEM. Asterisks indicate $p < 0.05$.

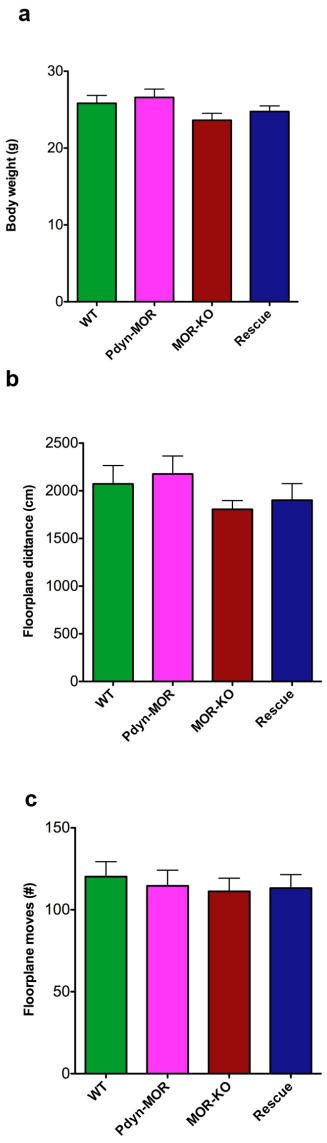


**Supplementary Figure S5.** *Pdyn-MOR* mice and *Rescue* mice do not exhibit significant deficits in body weight or locomotor behaviors. (**a**) The body weights of the *WT*, *Pdyn-MOR*, *MOR-KO* and *Rescue* mice are not significantly different ($F_{(3, 44)}$=1.864, $p$ = 0.1497, ANOVA, n = 12 for genotypes). (**b** and **c**) Locomotor activities in the open field test were obtained for adult *WT*, *Pdyn-MOR*, *MOR-KO* and *Rescue* mice (n=8 per genotype). No significant differences were observed in (**b** floorplane distance (cm) and (**c**) floorplane moves among the different genotypes. ($F_{(3, 28)}$ = 0.9993, $p$ = 0.2778 for floorplane distance; $F_{(3, 28)}$ = 0.2574, $p$ = 0.9061 for floorplane moves; One-Way ANOVA, n=8 for all groups)

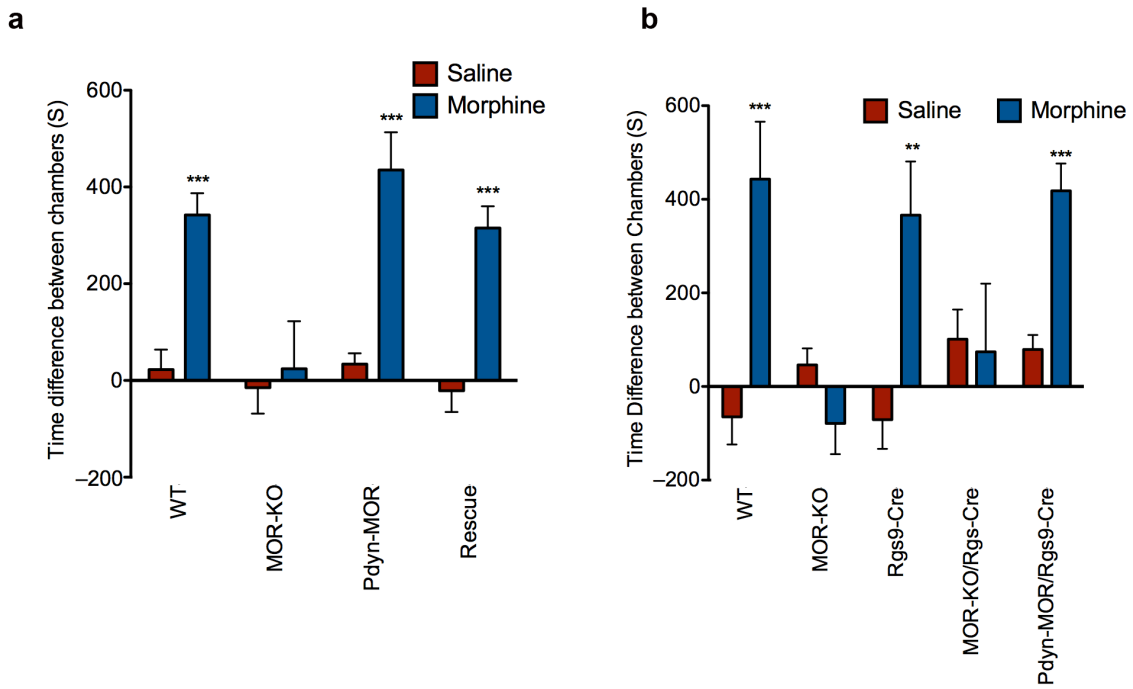


**Supplementary Figure S6** Morphine rewarding effect is rescued by *Pdyn-BAC*-driven expression of the MOR. (**a**) An independent cohort of mice are used to show that the CPP deficit in the *MOR-KO* mice is restored to the WT level in the *Rescue* mice. (genotype x $F_{(3, 41)}$=3.887, $p$ = 0.0156, genotype x treatment interaction, two way ANOVA; n=7, WT+morphine group; n=6 in all other groups). (**b**) The *Rgs9-Cre* transgene alone has no significant deficits in CPP ($F_{(4,71)}$=5,338, $p$ = 0.0008; genotype x treatment interaction, two way ANOVA, n=7-9 per group).The *WT*, *MOR-KO*, and *Rescue/Cre* mice are the same group of littermate mice as those shown in **Fig. 5b**. Values are mean ± SEM. Triple asterisk indicates $p < 0.001$.

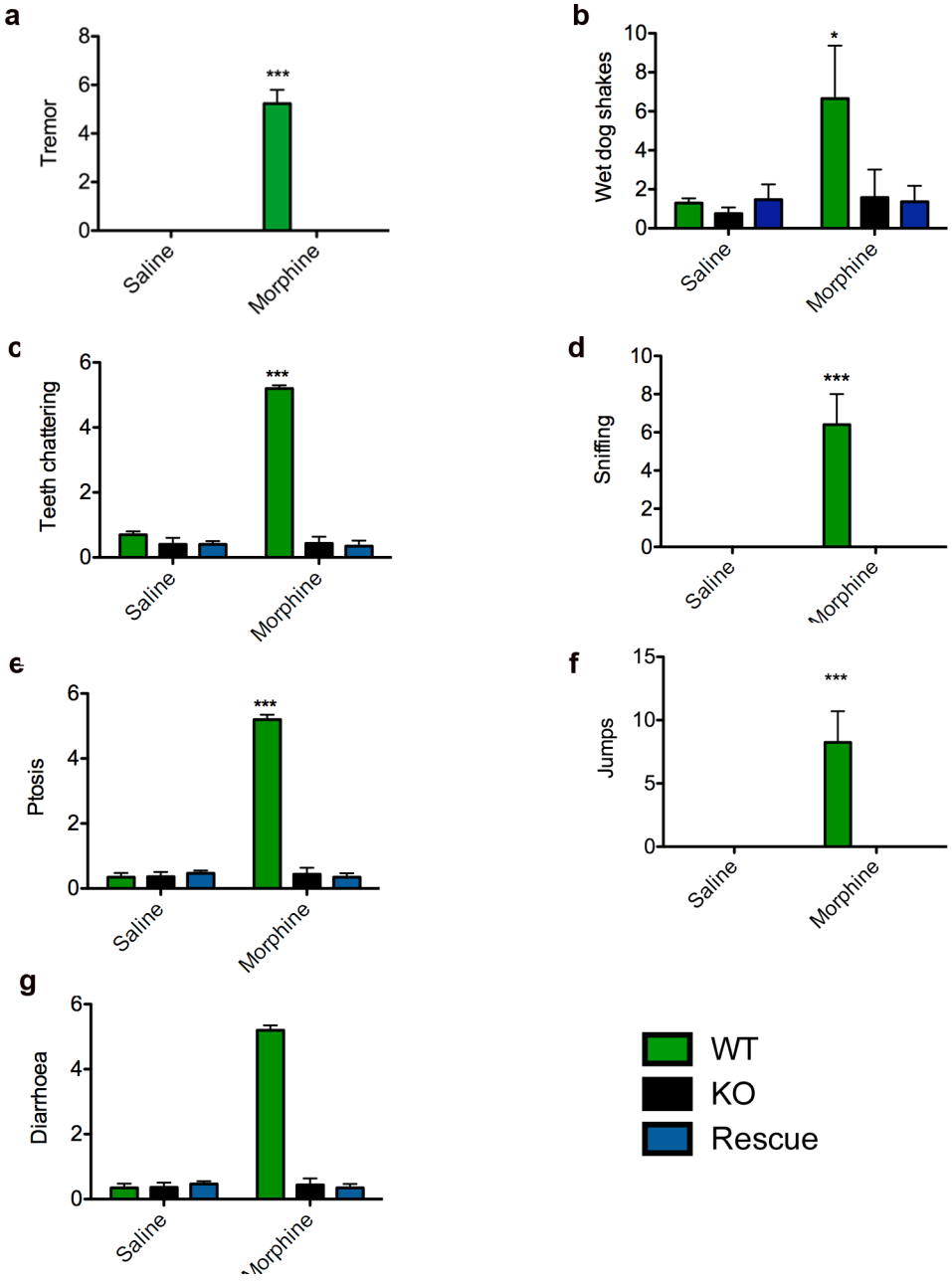


**Supplementary Figure S7.** Naloxone-precipitated morphine withdrawal syndrome is not significantly restored by *Pdyn-BAC* driven expression of MOR in the striatal direct-pathway MSN subpopulations. (**a**) tremor; (**b**) wet dog shakes; (**c**) teeth chattering; (**d**) sniffing; (**e**) ptosis; (**f**) jumping and (**g**) diarrhea. Results are expressed as means ± SEM. Triple asterisks indicate $p < 0.001$ and single asterisk indicates $p < 0.05$.

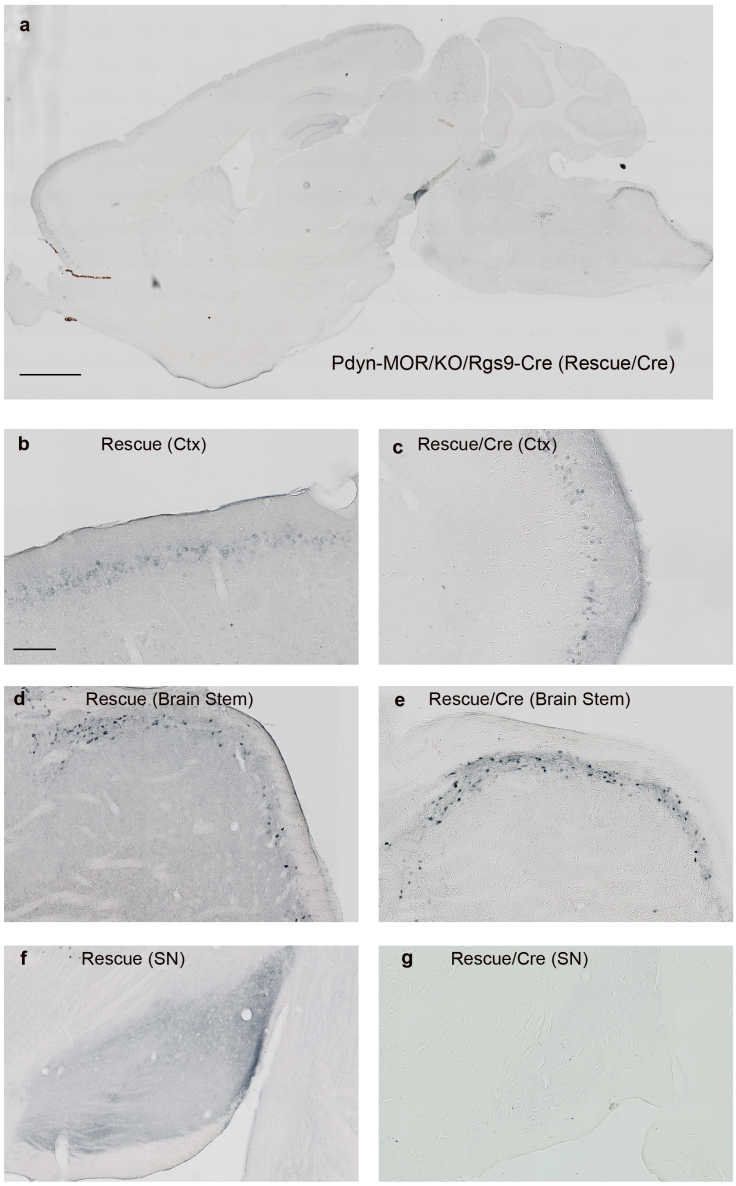


**Supplementary Figure S8**. Immunohistochemistry staining of MOR in *Rescue/Cre* and *Rescue* mice. (**a**). A low magnification image of *Rescue/Cre* mice showed the striatal MOR expression is abolished. (**b-g)** Higher magnificent images to compare MOR expression in *Rescue* mice (**b**,**d**,**f**) and *Rescue/Cre* mice (**c**,**e**,**g**) in the cortex (**b,c**), the brain stem (**d,e**) and substantia nigra (**f,g**). The result showed *Rgs9-Cre* can selectively remove in *Rescue/Cre mice* the expression of MOR in the striatal-direct pathway MSNs and their axonal terminals in SNc, but did not alter MOR expression in the cortex or brain stem compared to *Rescue* mice.

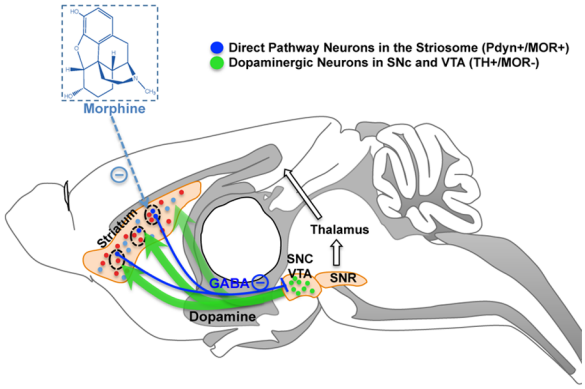


Supplementary Figure S9. The role of striatal direct-pathway MSNs in the striosome and NAc in regulating striatal dopamine release in our *Rescue* mice. MOR is selectively expressed in a subpopulation of striatal direct-pathway MSNs (black dotted circle) located in the striosome and NAc, which form monosynaptic inputs to the DA neurons in VTA and SNc. Opioids (*e.g.* morphine) binding to MOR on this direct-pathway MSN subpopulation results in the restoration of striatal dopamine release and opiate-driven reward and reinforcement behaviors in the *Rescue* mice.

**Supplementary Table S1: Oligonucleotide primers used in the study.**

| Gene | Primer name | Sequence (5'-3') |
|---|---|---|
| Pdyn-MOR transgene | Pdyn-MOR_F | AGTCCTTGGCCTTGACTCCTAGGTTCT |
| | Pdyn-MOR_R | GTCAGTTTCTTACAAGGACAAGCCC |
| mGAPDH | mGAPDH_F | TGTGTCCGTCGTGGATCTGA |
| | mGAPDH_R | CCTGCTTCACCACCTTCTTGA |
| | mGAPDH_P | (FAM)CCGCCTGGAGAAACCTGCCAAGTATG(TAMRA) |
| MOR (#1) | MOR(#1)_F | CCTGGAACCCGAACACTCTT |
| | MOR(#1)_R | GCTAAGGGGTCAGAGCAGTC |
| MOR (#2) | MOR(#2)_F | CACGTTGATGGCAACCAGTC |
| | MOR(#2)_R | CGTGCTAGTGGCTAAGGCAT |
| ß-Actin | ACT-B_F | ATGCTCCCCGGGCTGTAT |
| | ACT-B_R | CATAGGAGTCCTTCTGACCCATTC |
| Drd1 | Drd1_F | GGCCTCTTCCTGGTCAATC |
| | Drd1_R | GAGCGTAGTCTCCCAGATCG |
| Drd2 | Drd2_F | TGAACAGGCGGAGAATGG |
| | Drd2_R | CTGGTGCTTGACAGCATCTC |
| Darp-32 | Darpp-32_F | TCCTCCTTCCCCTACCAGTG |
| | Darpp-32_R | TCCTCCTTCCCCTACCAGTG |
| Pdyn | Pdyn_F | CATCCTGAATCCTCACTGCACA |
| | Pdyn_R | CTTCTGAATCTTGGATCGGCCA |